

Nitrogen and hydrological cycles under historical climate and land use

M. Lee et al.

Capturing interactions between nitrogen and hydrological cycles under historical climate and land use: Susquehanna watershed analysis with the GFDL Land Model LM3-TAN

M. Lee¹, S. Malyshev², E. Shevliakova², and P. R. Jaffé¹

¹Department of Civil and Environmental Engineering, Princeton University, Princeton, NJ, USA

²Princeton Environmental Institute, Princeton University, NOAA/Geophysical Fluid Dynamics Laboratory affiliate, Princeton, NJ, USA

Received: 24 February 2014 – Accepted: 21 March 2014 – Published: 16 April 2014

Correspondence to: M. Lee (minjinl@princeton.edu)

Published by Copernicus Publications on behalf of the European Geosciences Union.

Title Page

Abstract

Introduction

Conclusions

References

Tables

Figures



Back

Close

Full Screen / Esc

Printer-friendly Version

Interactive Discussion

Abstract

We developed a process model LM3-TAN to assess the combined effects of direct human influences and climate change on Terrestrial and Aquatic Nitrogen (TAN) cycling. The model was developed by expanding NOAA's Geophysical Fluid Dynamics Laboratory land model LM3V-N of coupled terrestrial carbon and nitrogen (C-N) cycling and including new N cycling processes and inputs such as a soil denitrification, point N sources to streams (i.e. sewage), and stream transport and microbial processes. Because the model integrates ecological, hydrological, and biogeochemical processes, it captures key controls of transport and fate of N in the vegetation-soil-river system in a comprehensive and consistent framework which is responsive to climatic variations and land use changes. We applied the model at $1/8^\circ$ resolution for a study of the Susquehanna River basin. We simulated with LM3-TAN stream dissolved organic-N, ammonium-N, and nitrate-N loads throughout the river network, and we evaluated the modeled loads for 1986–2005 using data from 15 monitoring stations as well as a reported budget for the entire basin. By accounting for inter-annual hydrologic variability, the model was able to capture inter-annual variations of stream N loadings. While the model was calibrated with the stream N loads only at the last downstream station Marietta (40.02° N, 76.32° W), it captured the N loads well at multiple locations within the basin with different climate regimes, land use types, and associated N sources and transformations in the sub-basins. Furthermore, the calculated and previously reported N budgets agreed well at the level of the whole Susquehanna watershed. Here we illustrate how point and non-point N sources contribute to the various ecosystems are stored, lost, and exported via the river. Local analysis for 6 sub-basins showed combined effects of land use and climate on the soil denitrification rates, with the highest rates in the Lower Susquehanna sub-basin (extensive agriculture; Atlantic coastal climate) and the lowest rates in the West Branch Susquehanna sub-basin (mostly forest; Great Lakes and Midwest climate). In the re-growing secondary forests, most of the N from non-point sources was stored in the vegetation and soil, but in the agricultural

BGD

11, 5669–5710, 2014

Nitrogen and hydrological cycles under historical climate and land use

M. Lee et al.

Title Page

Abstract

Introduction

Conclusions

References

Tables

Figures



Back

Close

Full Screen / Esc

Printer-friendly Version

Interactive Discussion

lands most N inputs were removed by soil denitrification indicating that anthropogenic N applications could drive substantial increase of N₂O emission, an intermediate of the denitrification process.

1 Introduction

Biologically available nitrogen (N) in terrestrial ecosystems has significantly increased via anthropogenic nutrient inputs: artificial fertilizer, cultivation of N fixing crops, and fossil fuel consumption (Galloway et al., 2004, 2008). This increase has caused acidification and N saturation in some terrestrial and aquatic ecosystems (Henriksen and Brakke, 1988; Kelly et al., 1990; Murdoch and Stoddard, 1992; Howarth, 2002). N-saturated soils and streams are also major sources of nitrous oxide (N₂O) emissions, which is a potent greenhouse gas (Albritton et al., 1994). Other concerns include severe water-quality problems associated with cultural eutrophication, which results in harmful algal blooms and hypoxia in rivers, lakes, estuaries, and coastal zone ecosystems (Smith, 2003; Smith et al., 2006). Climate change and variability also affect water quality through the distribution of high and low flow extremes (Scavia et al., 2002; Hawarth et al., 2006). It is generally accepted that microbial processes related to the N cycle are strongly influenced by abiotic factors, and warm or wet climate provides favorable environments for certain groups of bacterial activities. Quantification and management of the diverse and coupled effects of human activity and climate change on N cycling requires a comprehensive model of the relevant coupled processes that can support the design of optimal nutrient loading controls to maintain desirable water quality and terrestrial ecosystem integrity.

To characterize implications of human and climate driven perturbation in the global N cycling and its implication for water and air quality, the next-generation of N cycling models need to (1) be global, (2) account for changes in terrestrial and aquatic ecosystem structure and functioning, (3) represent in consistent manner emissions and transformation of N to air, rivers and coasts. Previously, none of the existing mod-

BGD

11, 5669–5710, 2014

Nitrogen and hydrological cycles under historical climate and land use

M. Lee et al.

Title Page

Abstract

Introduction

Conclusions

References

Tables

Figures

⏪

⏩

◀

▶

Back

Close

Full Screen / Esc

Printer-friendly Version

Interactive Discussion



Nitrogen and hydrological cycles under historical climate and land use

M. Lee et al.

Title Page

Abstract

Introduction

Conclusions

References

Tables

Figures

⏪

⏩

◀

▶

Back

Close

Full Screen / Esc

Printer-friendly Version

Interactive Discussion

processes; phenological leaf drop and its contribution to soil organic matter pools). INCA-N and SWAT are widely used Geographic Information System-based watershed models (Wade et al., 2002; Schilling and Wolter, 2009). However, when it comes to large scale applications, because these models are semi-distributed, they are less capable of representing spatial variability, requiring users to define the number and sizes of sub-basins, in which land use and all of the processes for each land use are assumed to be homogeneous and needed to be defined individually. This limits their ability to analyze complex land-use management scenarios. In this class of models, RHESSys is one of a few models with an ecology component that can be used to investigate interactions between ecosystems and hydrological processes according to climate variability (Tague and Band, 2004; Beckers et al., 2009). However, like the most models, because these models do not simulate vegetation and land use type distribution, a specific parameter set that describes typical soil, vegetation, and land use characteristics has to be developed using its special module when a study site requires different vegetation or soil types from its default application. This explains why RHESSys has only been applied to very small or sub sections of catchments (Band et al., 2001; Tague and Band, 2004).

Given the current lack of models that link terrestrial C-N cycling, long-term vegetation and land-use dynamics to N loads and concentrations in streams, accounting for different N species, the goal of this research was to build a model to simulate stream N loads that is based on a global-scale terrestrial and N-enabled land model, followed by its testing on a large and complex watershed, for which many years of stream discharge and stream N data are available. For this purpose and to assess the combined effects of direct human influences and climate change on Terrestrial and Aquatic Nitrogen (TAN) cycling, we developed a process model LM3-TAN. The new features include integrated effects of point and non-point sources on river N loads, a soil denitrification module, and stream microbial processes.

We applied LM3-TAN to the Susquehanna River basin, the largest of the watersheds in the northeastern US, draining an area of 71 220 km², at the resolution of 1/8°. The

model was evaluated using 20 year (1986–2005) data of stream ammonium (NH_4^+) and dissolved organic N loads as well as stream nitrate (NO_3^-) N loads from 15 monitoring stations. For each of 6 sub-basins, we conducted local analysis to assess combined effects of land use and climate on the soil denitrification. We then built up a N budget and compared it with the corresponding reported budget to better understand how point and non-point N sources contributed to the various ecosystems are stored, lost, and exported via the river at the level of the whole Susquehanna watershed. Although there are several parameters that required calibration by fitting simulated to observed stream N loads, these parameters are used universally for the entire basin where climate, soil, vegetation, and land use characteristics vary. Efforts have been made in the development of this model to limit the number of calibrated parameters.

2 Model description

2.1 Overview

LM3V-TAN is an expansion of earlier GFDL land models, beginning with LM3V of Shevliakova et al. (2009), which describes vegetation and C dynamics. LM3-TAN was expanded to include vegetation- and soil-N dynamics from LM3V-N (Gerber et al., 2010), new soil physics and hydrology from LM3 (Milly et al., 2014), and N cycling processes described here. LM3 was used as a component of the GFDL Earth System Models (Dunne et al., 2012) and included several enhancements, such as vertically resolved soil physics and hydrology and explicit river dynamics and physics. LM3-TAN includes soil denitrification and transport and chemistry of N cycle in rivers. This version of the model allows more complete tracking of N through the soil-river continuum. In this section, we first summarize key features of the model, and then we describe the newest N cycling features.

LM3V simulates distribution of five vegetation functional types (C3 and C4 grasses, and temperate-deciduous, tropical, and cold-evergreen trees) on the basis of total

BGD

11, 5669–5710, 2014

Nitrogen and hydrological cycles under historical climate and land use

M. Lee et al.

Title Page

Abstract

Introduction

Conclusions

References

Tables

Figures

⏪

⏩

◀

▶

Back

Close

Full Screen / Esc

Printer-friendly Version

Interactive Discussion



biomass and prevailing climate conditions. The model tracks hundreds of years of land use change using land use transition scenarios that were historically reconstructed (Hurt et al., 2006). The four land use types are natural vegetation (land undisturbed by human activities), secondary vegetation (land formerly disturbed by human activities), cropland, and pasture. The model is spatially distributed, and each grid cell consists of up to 15 tiles: 1 natural vegetation, 1 cropland, 1 pasture, and 1 to 12 secondary vegetation tiles representing unique disturbance histories. Exchanges of water, energy, and between land and atmosphere are computed with a time step of 30 minutes. Atmospheric and terrestrial reservoirs include C pools in vegetation (leaves, fine roots, sapwood, heartwood, and labile C storage), soil (fast and slow), and anthropogenic storage. The C pools in the vegetation are updated on a daily time step to account for vegetation growth and allocation, leaf drop and display, and natural mortality and fire. The soil C, which is supplied by the vegetation both naturally and during land-use conversion, is stored in two pools with different turnover times.

2.2 Coupled C-N dynamics in vegetation and soil

The previous two soil C pools in LM3V were divided into four pools (fast and slow litter, and slow and passive soil organic matter) in LM3V-N. Each C pool in the vegetation and soil was paired with a respective N compartment using pool-specific C : N ratios. The decomposition processes release biologically available forms of N (NO_3^- -N; NH_4^+ -N). This allows simulating N limitation on plant growth and biological N fixation as well as N feedbacks on organic matter decomposition and stabilization. Inorganic N is removed by sorption to soil particles, plant uptake, immobilization into long-lived organic compounds, and hydrological leaching, while organic N is lost through fire and hydrological leaching. Loss of nitrate N by soil denitrification was not differentiated from the hydrological nitrate-N leaching in LM3V-N.

BGD

11, 5669–5710, 2014

Nitrogen and hydrological cycles under historical climate and land use

M. Lee et al.

[Title Page](#)

[Abstract](#)

[Introduction](#)

[Conclusions](#)

[References](#)

[Tables](#)

[Figures](#)

[⏪](#)

[⏩](#)

[◀](#)

[▶](#)

[Back](#)

[Close](#)

[Full Screen / Esc](#)

[Printer-friendly Version](#)

[Interactive Discussion](#)

2.3 Improved soil and river physics and hydrology

LM3 introduced vertically distributed soil-water, soil-ice and temperature profiles extending many meters below the surface, but with high resolution (thinnest layer 0.02 m) near the surface. Water (potentially) discharges laterally from each soil layer to the local river reach. Each horizontal grid cell of the model contains only one river reach, and each reach discharges to another reach in the downstream grid cell, following a network that ultimately discharges to the ocean; the sub-grid-scale stream network is ignored. Relations among discharge, storage, velocity, width, and depth in each reach are specified according to Leopold and Maddock (1953).

2.4 Synthesis and extension of earlier developments

For this study, we first combined the lumped N model LM3V-N with the distributed physics of LM3. To complete the N mass balance, we next added a soil denitrification module. Finally, we added stream transport and microbial processes to track the fate of soil N leaching and resolve N dynamics in the aquatic ecosystem. Each of these steps is described below. Figure 1 shows stores and fluxes of N in the resultant model, along with relevant processes. Newly introduced or adjusted parameters from the earlier developments are summarized in Table 1 and variables are listed in Table 2.

2.4.1 Merging lumped N model with distributed physical model

To account for dependence of processes in the lumped soil C and N pools upon the vertically resolved physical states of the soil (temperature and water content), the latter were vertically averaged with an exponentially decaying weight function of depth (e-folding depth of 10 m). Leaching of any mobile constituent was defined as the product of a concentration and the sum of lateral and vertical discharge from the soil layer between the surface and a depth of 10 m. The concentration of available N was calculated as dividing available N contents by the effective soil depth which was approximated as-

BGD

11, 5669–5710, 2014

Nitrogen and hydrological cycles under historical climate and land use

M. Lee et al.

Title Page

Abstract

Introduction

Conclusions

References

Tables

Figures

⏪

⏩

◀

▶

Back

Close

Full Screen / Esc

Printer-friendly Version

Interactive Discussion

suming C weight content 3.4% and average soil density 1500 kg m^{-3} . The available N refers to the N contents reduced by buffering factors which represent processes such as sorption to soil particles. To compensate for many processes that were not accounted for in the model, calibration factors for each N species were introduced to slow down overall N movement from the soil to the stream. These factors include impacts of soil microbes, which are able to take up and incorporate all N forms (NO_3^- -N, NH_4^+ -N, DON) with a much greater capacity than plant uptake (Nordin et al., 2004). The nitrate calibration factor also accounts for storage in groundwater since nitrate (the primary form of N in ground water) can persist for decades at high levels with increasing N applications. This is further explained by Bachman et al. (1998) which reported that 17 to 80 % of the N delivered to streams of the Chesapeake Bay watershed was through ground water. Furthermore, the lumped single-layer N sub-model bypasses most of the vertically distributed hydrologic system, and the soil N leaching based on the average water drainage is transferred directly from the N layer into the stream. These calibration factors were fit to match inter-annual variations of observed and simulated stream N loads to make up for this modeling approach as well as the unresolved processes that might cause inter-annual stream N loads more sensitive to climate variability than those in reality. The need to incorporate these calibration factors indicates that future improvements to LM3-TAN should focus on resolving these processes.

$$L_{\text{DON}} = \frac{D_s}{\rho_w r_{\text{DOM}}} [N_{\text{DON}, \text{av}}] = \frac{D_s}{\rho_w r_{\text{DOM}}} \left(\frac{f_{\text{LF}} N_{\text{LF}} + f_{\text{LS}} N_{\text{LS}} + f_{\text{SS}} N_{\text{SS}}}{b_{\text{DOM}} h_s} \right) \quad (1)$$

$$L_{\text{NH}_4^+} = \frac{D_s}{\rho_w r_{\text{NH}_4^+}} [N_{\text{NH}_4^+, \text{av}}] = \frac{D_s}{\rho_w r_{\text{NH}_4^+}} \left(\frac{N_{\text{NH}_4^+}}{b_{\text{NH}_4^+} h_s} \right) \quad (2)$$

$$L_{\text{NO}_3^-} = \frac{D_s}{\rho_w r_{\text{NO}_3^-}} [N_{\text{NO}_3^-, \text{av}}] = \frac{D_s}{\rho_w r_{\text{NO}_3^-}} \left(\frac{N_{\text{NO}_3^-}}{b_{\text{NO}_3^-} h_s} \right) \quad (3)$$

$$h_s = \frac{C_{\text{LF}} + C_{\text{LS}} + C_{\text{SS}}}{r_c \rho_s} \quad (4)$$

Nitrogen and hydrological cycles under historical climate and land use

M. Lee et al.

Title Page

Abstract

Introduction

Conclusions

References

Tables

Figures

⏪

⏩

◀

▶

Back

Close

Full Screen / Esc

Printer-friendly Version

Interactive Discussion



Nitrogen and hydrological cycles under historical climate and land use

M. Lee et al.

Title Page

Abstract

Introduction

Conclusions

References

Tables

Figures

⏪

⏩

◀

▶

Back

Close

Full Screen / Esc

Printer-friendly Version

Interactive Discussion



where, L_{DON} , $L_{\text{NH}_4^+}$, and $L_{\text{NO}_3^-}$ are the dissolved organic, ammonium, and nitrate N leaching from the soil ($\text{kg m}^{-2} \text{s}^{-1}$); D_s is the water drainage from the active soil layer ($\text{kg m}^{-2} \text{s}^{-1}$); ρ_w is the water density (1000 kg m^{-3}); r_{DOM} , $r_{\text{NH}_4^+}$, and $r_{\text{NO}_3^-}$ are dissolved organic matter, ammonium, and nitrate N calibration factors; $[N_{\text{DON, av}}]$, $[N_{\text{NH}_4^+, \text{av}}]$, and $[N_{\text{NO}_3^-, \text{av}}]$ are the concentration of available N in dissolved organic, ammonium, and nitrate N pools (kg m^{-3}); N_{LF} , N_{LS} , and N_{SS} are the fast litter, slow litter, and slow soil N contents (kg m^{-2}); f_{LF} , f_{LS} , and f_{SS} are the fractions of soluble organic N in the fast litter, slow litter, and slow soil N pools; $N_{\text{NH}_4^+}$ and $N_{\text{NO}_3^-}$ are the soil ammonium and nitrate N contents (kg m^{-2}); b_{DOM} , $b_{\text{NH}_4^+}$, and $b_{\text{NO}_3^-}$ are dissolved organic matter, ammonium, and nitrate N buffering factors due to sorption to soil particles; h_s is the effective soil depth (m); r_c is the C weight content (3.4%); ρ_s is the average soil density (1500 kg m^{-3}); C_{LF} , C_{LS} , and C_{SS} are the fast litter, slow litter, and slow soil C contents (kg m^{-2}).

2.4.2 Denitrification in soil

Denitrification is a process that reduces nitrate or nitrite to gaseous forms (e.g., NO , N_2O , N_2) in anaerobic conditions, where the oxidized N species serve as a terminal electron acceptor in metabolism by soil denitrifying bacteria. The rate of denitrification generally depends on soil nitrate content or concentration, soil water content (a surrogate for oxygen content), and soil temperature. Because soil nitrate contents are relatively low and limiting under natural conditions, we used a first-order loss function with respect to soil nitrate N content, with adjustments for the influence of soil water content and temperature.

$$D_{\text{N}} = f_{\text{S}} f_{\text{T}} k_{\text{denitr}} N_{\text{NO}_3^-} \quad (5)$$

where, D_{N} is the soil denitrification rate ($\text{kg m}^{-2} \text{ yr}^{-1}$); f_{S} is a soil water content reduction function; f_{T} is a soil temperature reduction function; k_{denitr} is a first-order denitrification

coefficient (yr^{-1}); $N_{\text{NO}_3^-}$ is the soil nitrate N content (kg m^{-2}).

$$f_T = Q_{10}^{(T-T_r)/T_p} \quad (6)$$

$$f_S = \begin{cases} S_{\min} & S < S_t \\ \left(\frac{S-S_t}{S_{\max}-S_t} \right)^w & S_t \leq S \leq S_{\max} \\ S_{\max} & S_{\max} < S \end{cases} \quad (7)$$

5 where, T is the soil temperature ($^{\circ}\text{C}$); T_r is a reference temperature ($^{\circ}\text{C}$); T_p is a parameter; Q_{10} is a factor change in rate with a 10° change in temperature; S is the soil water content; S_t is a threshold soil water content; S_{\max} is the maximum soil water content; S_{\min} is the minimum soil water content; w is an empirical constant.

Heinen (2006) tabulates reported values of the various parameters introduced above.
 10 Figure 2 shows the effects of the reduction functions on the soil denitrification rate that were applied in diverse models as well as LM3-TAN. Figure 2a shows how fast soil nitrate N content is reduced to half of the initial amount depending on the different first-order denitrification coefficients. As temperature increases the bacterial activities increase exponentially (Fig. 2b). Soil denitrification occurs and increases non-linearly
 15 only if soil water content exceeds a certain threshold point due to enhanced anaerobic bacterial activity (Fig. 2c). The soil water content reduction function for other microbial processes (e.g., mineralization, nitrification) used in LM3-TAN is also shown in Fig. 2d. Because k_{denitr} is by far the most widely used parameter of these, with reported values ranging over three orders of magnitude, our strategy was to fix the other parameters
 20 using reported values, and to calibrate the model by determining k_{denitr} within the bounds reported in the literatures. Because soil denitrification and nitrate-N leaching are competing sinks of nitrate N in the soil, soil denitrification increases as soil nitrate-N leaching or stream nitrate-N load decreases; thus k_{denitr} was fit to match observed and simulated stream nitrate-N loads.

Nitrogen and hydrological cycles under historical climate and land use

M. Lee et al.

Title Page	
Abstract	Introduction
Conclusions	References
Tables	Figures
⏪	⏩
◀	▶
Back	Close
Full Screen / Esc	
Printer-friendly Version	
Interactive Discussion	



Nitrogen and hydrological cycles under historical climate and land use

M. Lee et al.

[Title Page](#)

[Abstract](#)

[Introduction](#)

[Conclusions](#)

[References](#)

[Tables](#)

[Figures](#)

[⏪](#)

[⏩](#)

[◀](#)

[▶](#)

[Back](#)

[Close](#)

[Full Screen / Esc](#)

[Printer-friendly Version](#)

[Interactive Discussion](#)



The wide ranges of the functions discussed above are mostly driven by the dependencies of the parameters on specific regions (with different soil properties, vegetation, land use, etc.). Given a number of proposed individual functions, it seems that there is no universal process module to simulate soil denitrification. Because such reduction functions display a diversity of shapes as ecosystems are modeled over a range of climate patterns, vegetation type, and land use practices, soil denitrification on a large scale cannot be modeled without proper adjustments that compensate the site-specific properties. This explains why only a few studies have applied models to watersheds larger than 1000 km² despite the diversity of existing dynamic N models and why semi-distributed models often parameterize these individual functions for each of sub-basins in large-scale applications. We hypothesize that LM3-TAN's integrated modeling framework, which is capable of simulating long-term vegetation functional type and land use change as a function of changes in CO₂, climate, and human influences, allows us to use a universal parameter set to simulate soil denitrification for each of the distinct sub-basins.

2.4.3 Microbial processes in rivers

Despite its importance to water quality, processes that control N removal from water bodies are rarely resolved in watershed scale models, due to both uncertainties in measurement techniques and lack of measurements. To date, none of studies focusing on river denitrification rate is based on measurements of an entire river network, but rather only on the data from low order streams or individual catchments. Here we applied a non-linear regression function based on the LINX (Lotic Intersite Nitrogen experiment; Mulholland et al., 2008) reach-scale measurements that correlates river denitrification rate with nitrate-N concentration and river depth to estimate the reaction rate constant of river denitrification for each reach (Alexander et al., 2009). The measured reaction rate constants vary from 0.034 to 117 (day⁻¹), and we chose the median value 0.53 (day⁻¹) as the minimum reaction rate constant of river denitrification. Eq. (12) indicates that the reaction rate constant decreases with increase in nitrate-N

concentration and river depth, since both b_1 and b_2 are negative, and it increases with temperature. Reaction rate constants for river mineralization and nitrification were calibrated to match stream N loads.

Figure 1 shows structure of the river component. Each reach directly receives N from point sources (e.g., sewage and waste water discharge) and indirectly receives N from non-point sources (e.g., atmospheric deposition, fertilizer, manure, and legume applications) via soil leaching. The N loads in a reach are routed downstream with the water.

$$\frac{dR_{\text{DON}}}{dt} = F_{\text{DON}}^{\text{in}} - F_{\text{DON}}^{\text{out}} + L_{\text{DON}} + P_{\text{DON}} - f_T' k_{\text{min}}' R_{\text{DON}} \quad (8)$$

$$\frac{dR_{\text{NH}_4^+}}{dt} = F_{\text{NH}_4^+}^{\text{in}} - F_{\text{NH}_4^+}^{\text{out}} + L_{\text{NH}_4^+} + P_{\text{NH}_4^+} + f_T' k_{\text{min}}' R_{\text{DON}} - f_T' k_{\text{nitr}}' R_{\text{NH}_4^+} \quad (9)$$

$$\frac{dR_{\text{NO}_3^-}}{dt} = F_{\text{NO}_3^-}^{\text{in}} - F_{\text{NO}_3^-}^{\text{out}} + L_{\text{NO}_3^-} + P_{\text{NO}_3^-} + f_T' k_{\text{nitr}}' R_{\text{NH}_4^+} - f_T' k_{\text{denitr}}' R_{\text{NO}_3^-} \quad (10)$$

$$f_T' = T_p' (T' - T_r') \quad (11)$$

$$k_{\text{denitr}}' = \max \left\{ k_{\text{denitr, min}}', C_{\text{d,s}} \left(b_0 C_{\text{NO}_3^-}^{b_1} H^{b_2} c^t \right) \right\} \quad (12)$$

where, i is DON , NH_4^+ , or NO_3^- ; R_i is the river N (kg m^{-2}); F_i^{in} and F_i^{out} is the inflow and outflow of the river N ($\text{kg m}^{-2} \text{s}^{-1}$); L_i is the N leaching from the soil ($\text{kg m}^{-2} \text{s}^{-1}$); P_i is the N point source ($\text{kg m}^{-2} \text{s}^{-1}$); f_T' is the stream temperature reduction function; T' is the water temperature ($^{\circ}\text{C}$); T_r' is the reference water temperature ($^{\circ}\text{C}$); T_p' is a parameter; k_{min}' , k_{nitr}' , and k_{denitr}' are the reaction rate constants for river mineralization, nitrification, and denitrification (s^{-1}); $k_{\text{denitr, min}}'$ is the minimum reaction rate constant of river denitrification (s^{-1}); $C_{\text{NO}_3^-}$ is the nitrate N concentration ($\mu\text{mol NL}^{-1}$); H is the river depth (m); b_0 , b_1 , and b_2 are the constants; c^t is the log re-transform bias correction factor; $C_{\text{d,s}}$ is a unit-conversion constant.

3 Study site

The Susquehanna River basin, where nearly four million people live, is the largest of the watersheds in the northeastern US and drains an area of 71 220 km², contributing two-thirds of the annual N load to the Chesapeake Bay (Fig. 3). The basin includes 2293 lakes, reservoirs, and ponds (322 km²) as well as 50 190 km of rivers and streams. The main stem of the Susquehanna River originates at Otsego Lake, N.Y., and flows about 750 km through New York, Pennsylvania, and Maryland to the Chesapeake Bay at Havre de Grace, Md. The Susquehanna Large River Assessment Project reported that only 6.9% of water quality values exceeded their standards, but the majority of these exceedances were for nutrients (e.g. TN, TP) (Hoffman, 2009), explaining why the Chesapeake Bay suffers from nutrient enrichment problems and hypoxia.

The reported 2000 land use is about 63% forest or wooded, 19% crop land, 7% pasture, 9% urban, and 2% water. The Upper Susquehanna River flows through mostly forested and agricultural land with some small communities and one larger population center, then confluences with the Chemung River at Sayre, Pa. The West Branch Susquehanna sub-basin is mostly woods and grasslands. The Middle Susquehanna River, from the confluences with the Chemung River at Sayre, Pa. to the confluences with the West Branch Susquehanna River at Sunbury, Pa., flows along very diverse land use. The Lower Susquehanna sub-basin contains extensive agriculture and several large population centers. The other major urban areas are found within the Juniata sub-basin (Hoffman, 2008).

The geology of the watershed is mainly classic sedimentary rock of sandstone and shale. Elevations vary from 30 m at the Chesapeake Bay in Maryland to 955 m in central New York State (McGonigal, 2011). The Great Lakes and Midwest climate exert influence over the Upper Susquehanna, Chemung, and West Branch Susquehanna sub-basin, whereas the Atlantic coastal climate affect on the other portions of the watershed. The basin has experienced severe droughts about once every decade, and the worst droughts occurred in 1930, 1939 and 1964. The basin is also one of the most

Nitrogen and hydrological cycles under historical climate and land use

M. Lee et al.

Title Page

Abstract

Introduction

Conclusions

References

Tables

Figures



Back

Close

Full Screen / Esc

Printer-friendly Version

Interactive Discussion



flood-prone watersheds in the nation with frequent and localized flash floods every year. The worst recorded flooding in the basin happened in 1972 as a result of tropical storm Agnes.

4 Stream sampling description

5 Stream discharge data are provided by the network of stream gages operated by the US Geological Survey (USGS), which collects and summarizes time series data to derive annual, monthly, and daily stream discharge and statistics (Fig. 3). Chemical constituents of the basin's water were monitored by the Susquehanna River Basin Commission (SRBC). Six long-term nutrient monitoring sites, monitored since 1985 and 9 newly introduced sites monitored since either 2004 or 2005 to present (Table 1; Fig. 3; McGonigal, 2011) were chosen for model evaluation. The 15 sites vary in sub-basin area and land use. The Marietta site on the main channel of the Susquehanna River has the largest sub-basin area (67 314 km²). The sub-basin of the Conestoga site contains extensive agriculture (48 %) and the most populated urban land use with several large population centers (24 %) within a very small area (1217 km²). The West Branch River flows mostly along woods and grasslands to the Lewisburg site. The 6 long-term sites have collected two samples per month. Additional samplings are made during seasonal storm conditions. The collected water samples are analyzed for various N species: dissolved N (DN), dissolved nitrite and nitrate (DNO₂₃), dissolved ammonia (DNH₃), dissolved organic N (DON), and dissolved ammonia and organic N (DKN) in milligrams per liter. In addition, annual, seasonal, and monthly loads are computed by the Minimum Variance Unbiased Estimator (ESTIMATOR; SRBC). River temperatures were reported when the samplings were collected for the chemical analysis of stream waters.

Nitrogen and hydrological cycles under historical climate and land use

M. Lee et al.

Title Page

Abstract

Introduction

Conclusions

References

Tables

Figures



Back

Close

Full Screen / Esc

Printer-friendly Version

Interactive Discussion



5 Anthropogenic N sources

Anthropogenic N data over the two decades (1985–2005) were provided by the Chesapeake Community Modeling Program (CCMP). Atmospheric deposition data were provided by the county-based land segments. Fertilizer, manure, and legume applications as well as combined sewer overflows (CSOs) were provided by the land-river segments of the GIS-based Phase 5.3 Community Watershed Model (USEPA, 2010a). The atmospheric deposition data were calculated by the Chesapeake Bay Program (CBP) Airshed Model, which is a combination of a regression model of wet deposition (Grimm and Lynch, 2005) and the Community Multiscale Air Quality Model (CMAQ) that estimates dry deposition (Dennis et al., 2007; Hameedi et al., 2007). The fertilizer, manure, and legume data were estimated for the years of 1985, 1987, 1992, 1997, 2002, and 2005 by the Scenario Builder Version 2.2, a process based model that is designed to use agricultural censuses as a main input data (USEPA, 2010b). The agricultural censuses were produced by the United States Department of Agriculture National Agricultural Statistics Service (NASS) and include data of animal populations, farms, agricultural land areas, and crop yields. The point sources were estimated by 42 CSO communities within the Susquehanna basin, using either various versions of EPA's Storm Water Management Model (SWMM) or spatial data collected as a result of a direct survey of the communities (USEPA, 2010a). The detailed data description can be found in the Phase 5.3 Community Watershed Model documentation (USEPA, 2010a).

Over the two decades, the total N sources decreased by about 20%. The atmospheric deposition was predominantly nitrate-N accounting for about 69%; ammonium-N 27%; organic-N 4%. The sum of the fertilizer, manure, and legume applications consisted of 49% of ammonium-N, followed by 37% organic-N, and 14% nitrate-N. Especially, the ammonium-N and organic-N loads had considerable variability across the spatial domain because they were strongly influenced by local emissions from the extensive agricultural areas.

Nitrogen and hydrological cycles under historical climate and land use

M. Lee et al.

Title Page

Abstract

Introduction

Conclusions

References

Tables

Figures



Back

Close

Full Screen / Esc

Printer-friendly Version

Interactive Discussion



Nitrogen and hydrological cycles under historical climate and land use

M. Lee et al.

[Title Page](#)

[Abstract](#)

[Introduction](#)

[Conclusions](#)

[References](#)

[Tables](#)

[Figures](#)

[⏪](#)

[⏩](#)

[◀](#)

[▶](#)

[Back](#)

[Close](#)

[Full Screen / Esc](#)

[Printer-friendly Version](#)

[Interactive Discussion](#)



Figure 4 shows spatial distribution maps of the applied anthropogenic N sources, which were calculated as a spatial resolution of 0.125° by 0.125° and a temporal resolution of one year. For each grid cell, which consists of up to 15 land-use tiles, atmospheric depositions (nitrate-N, ammonium-N, and organic-N) were applied to all of the land tiles, and fertilizer, manure, and legume applications (nitrate-N, ammonium-N, and organic-N) were applied only to the crop land tiles. Combined sewer overflows (nitrate-N, ammonium-N, and organic-N) were directly applied to the river reaches. The 20-year (1986–2005) average non-point and point N sources for the six sub-basins are summarized in the Table 4. The thick solid arrows in Fig. 1 depict fluxes of each of N species for the anthropogenic N sources to the corresponding terrestrial and river pools respectively.

6 Model forcing and simulations

The model was implemented with a spatial resolution of 0.125° by 0.125° with time increments of 30 min. The model was forced using observed hydrological data cycled over a horizon of 61 years (1948–2008) to perform long-term simulations. The data include precipitation, specific humidity, air temperature, surface pressure, wind speed, and short and long wave downward radiation with a spatial resolution of 1° by 1° on timescales of 3 hours (Sheffield et al., 2006). Land-use change was simulated from 1704 to 2005 using a scenario of land use transitions (Hurtt et al., 2006). Preindustrial CO_2 concentration assumed as 286 ppm was applied from 1704 to 1799, and changes in CO_2 concentrations were applied from 1800 to 2005 using an observed data from NOAA's Earth System Research Laboratory. For 250 years (1704–1953), the estimated preindustrial N deposition (Dentener and Crutzen, 1944; Green et al., 2004; Gerber et al., 2010) was applied as a uniform annual rate. We then applied the reported 1985's data from 1954 to 1984, and annual anthropogenic N data from 1985 to 2005.

7 Result and discussion

7.1 Evaluation of stream waters and N loads

Stream discharges as well as stream nitrate, ammonium, and dissolved organic N loads were evaluated using 20 year (1986–2005) river data from the 15 monitoring stations. For time series analysis, we focused on the evaluation at the last downstream station Marietta, in which contributions of the entire watershed to the stream flows and N loads can be assessed. In general, the model had an ability to produce temporal patterns of annual stream discharge ($R^2 = 0.6$). The simulated flows were in a good agreement with the observed flows in dry years, but under-estimated in wet years. A good fit was obtained for monthly average flows during the dry period (July to September), though they were under-estimated in the wet period (March to May). Overall, 19 year average simulated flow was about 28 % lower than the corresponding reported value. Simulated river temperatures were close to the corresponding monitored data ($R^2 \cong 0.9$).

Due to their complex physical and biogeochemical interactions with soil particles and soil organic matter, simulating reactive transport of ammonium and dissolved organic N is far more challenging than simulating nitrate N transport. For example, the correlation at Marietta between stream discharge and nitrate N ($R^2 = 0.98$) was significantly higher than that for dissolved organic N ($R^2 = 0.48$) or for ammonium N ($R^2 = 0.85$), implying that in addition to the hydrological processes governing soil N transport to rivers, terrestrial physical and microbial processes (e.g., sorption to soil particles, organic matter decomposition and stabilization) have to be accounted for when estimating stream ammonium and dissolved organic N loads. This, plus the fact that the highest component in the overall stream N load is nitrate N, explains why existing watershed models have focused on stream nitrate N loads, and neglected ammonium and dissolved organic N loads. Within the LM3-TAN's integrated modeling framework, we estimated all of the N species for the entire drainage network.

At Marietta, 19 year average simulated stream dissolved-N (−0.5%), nitrate-N (−0.2%), ammonium-N (+4.7%), and dissolved organic-N (−2.6%) loads were close

Nitrogen and hydrological cycles under historical climate and land use

M. Lee et al.

[Title Page](#)

[Abstract](#)

[Introduction](#)

[Conclusions](#)

[References](#)

[Tables](#)

[Figures](#)

[⏪](#)

[⏩](#)

[◀](#)

[▶](#)

[Back](#)

[Close](#)

[Full Screen / Esc](#)

[Printer-friendly Version](#)

[Interactive Discussion](#)

- On a sub-basin scale with different climate and land-use regimes, the LM3-TAN properly simulates terrestrial N cycling, including effects of long-term vegetation dynamics, land-use changes, and hydrological cycles. The interaction among those three processes allow LM3-TAN to capture soil C-N organic matter and mineral N transformations as well as soil emissions of nitrate-N and leaching of dissolved organic, ammonium, and nitrate N.
- The ability to capture N soil budget and losses then enables LM3-TAN to consistently characterize trends and variability in riverine N inputs and exports of ammonium, dissolved organic, and nitrate N with explicit representation of their transformations and transport in rivers.
- LM3-TAN captures effects of long-term trends and variability of hydrological cycles (e.g., precipitation, soil water content, stream discharge) on N cycling in vegetation-soil-river system, and thus resolving inter-annual variations of stream N loadings caused by climate variability.
- In the re-growing secondary forests, a large fraction of the N from atmospheric deposition has been stored in the vegetation and soil, but in the agricultural lands most N inputs were removed by soil denitrification indicating that anthropogenic N inputs could drive substantial increase of N_2O emission, an intermediate of the denitrification process.
- The model results suggest that the soil denitrification is sensitive the most to soil water variations.
- Among the 6 sub-basins, the soil denitrification rate was the highest in the Lower Susquehanna sub-basin with the most intensive land-use non-point N sources as well as with the warmest and wettest soils, attributed to the Atlantic coastal climate.
- Even though the N denitrification and riverine biogeochemistry N modules were calibrated only at the last downstream station Mariette, application of the universal

parameters at the entire watershed produced simulations which compared well at other observational stations. The applicability of the universal parameters in other watersheds is a subject of the future research.

- This study shows that linking terrestrial N and C cycling, long-term land-use and vegetation dynamics, and hydro-climate variations to N loads and concentrations in streams, provides an effective and consistent framework for analysis of the surface water N processes and water quality for large watersheds and basins.

Acknowledgements. We thank P. C. D. Milly and Krista A. Dunne of the United States Geological Survey for help and advise in using and interpreting hydrologic module of LM3-TAN, including creation of the 1/8° river network dataset.

Support for M. Lee was provided by a Fulbright Scholarship, by the Princeton Environmental Institute at Princeton University through the Mary and Randall Hack '69 Research Fund, and by the Korean National Institute of Environmental Research.

References

- Albritton, D. L., Derwent, R. G., Isaksen, I. S. A., Lal, M., and Wuebles, D. J.: Trace gas radiative forcing indices, in: *Climate Change 1994: Radiative Forcing of Climate Change and an Evaluation of the IPCC IS92 Emission Scenarios*, edited by: Houghton, J. T., Cambridge University Press, Cambridge, UK, 205–231, 1995.
- Alexander, R. B., Bohlke, J. K., Boyer, E. W., David, M. B., Harvey, J. W., Mulholland, P. J., Seitzinger, S. P., Tobias, C. R., Tonitto, C., and Wollheim, W. M.: Dynamic modeling of nitrogen losses in river networks unravels the coupled effects of hydrological and biogeochemical processes, *Biogeochemistry*, 93, 91–116, 2009.
- Bachman, L. J., Lindsey, B. D., Brakebill, J. W., and Powars, D. S.: Ground-water discharge and base-flow nitrate loads of non tidal streams, and their relation to a hydrogeomorphic classification of the Chesapeake Bay watershed, *US Geological Survey Water-Resources Investigations Rep. 98–4059*, 71 pp., 1998.
- Band, L. E., Tague, C. L., Groffman, P., and Belt, K.: Forest ecosystem processes at the watershed Scale: hydrological and ecological controls of nitrogen export, *Hydrol. Process.*, 15, 2013–2028, 2001.

Nitrogen and hydrological cycles under historical climate and land use

M. Lee et al.

Title Page

Abstract

Introduction

Conclusions

References

Tables

Figures



Back

Close

Full Screen / Esc

Printer-friendly Version

Interactive Discussion



Nitrogen and hydrological cycles under historical climate and land use

M. Lee et al.

[Title Page](#)

[Abstract](#)

[Introduction](#)

[Conclusions](#)

[References](#)

[Tables](#)

[Figures](#)

[⏪](#)

[⏩](#)

[◀](#)

[▶](#)

[Back](#)

[Close](#)

[Full Screen / Esc](#)

[Printer-friendly Version](#)

[Interactive Discussion](#)



- Beckers, J., Smerdon, B., and Wilson, M.: Review of hydrologic models for forest management and Climate change applications in British Columbia and Alberta, FORREX SERIES 25, FORREX Forum for Research and Extension in Natural Resources Society, Kamloops, B. C., 2009.
- 5 Bolker, B. M., Pacala, S. W., and Parton, W. J.: Linear analysis of soil decomposition: insights from the CENTURY model, *Ecol. Appl.*, 8, 425–439, 1998.
- Boyer, E. W., Goodale, C. L., Jaworski, N. A., and Howarth, R. W.: Anthropogenic nitrogen sources and relationship to riverine nitrogen export in the northeastern USA., *Biogeochemistry*, 57–58, 137–169, 2002.
- 10 Bril, J., van Faassen, H. G., and Klein Gunnewiek, H.: Modeling N₂O Emission from Grazed Grassland, Report 24, Institute for Agrobiology and Soil Fertility, Wageningen, the Netherlands, 1994.
- Chesapeake Community Modeling Program: available at: <http://ches.communitymodeling.org/index.php> (last access: 17 January 2014), 2010.
- 15 Del Grosso, S. J., Ojima, D. S., Parton, W. J., Stehfest, E., Heistemann, M., DeAngelo, B., and Rose, S.: Global scale DAYCENT model analysis of greenhouse gas emissions and mitigation strategies for cropped soils, *Global Planet. Change*, 67, 44–50, 2009.
- Dennis, R., Haeuber, R., Blett, T., Cosby, J., Driscoll, C., Sickles, J., and Johnson, J.: Sulfur and nitrogen deposition on ecosystems in the United States, *EM: The Magazine for Environmental Managers*, December 2007, 12–17, 2007.
- 20 Dentener, F. J. and Crutzen, P. J.: A three-dimensional model of the global ammonia cycle, *J. Atmos. Chem.*, 19, 331–369, 1994.
- Dunne, J. P., John, J. G., Adcroft, A. J., Griffies, S. M., Hallberg, R. W., Shevliakova, E., Stouffer, R. J., Cooke, W., Dunne, K. A., Harrison, M. J., Krasting, J. P., Malyshev, S. L., Milly, P. C. D., Phillipps, P. J., Sentman, L. T., Samuels, B. L., Spelman, M. J., Winton, M., Wittenberg, A. T., and Zadeh, N.: GFDL's ESM2 global coupled climate-carbon Earth System Models. Part I: Physical formulation and baseline simulation characteristics, *J. Climate*, 25, 6646–6665, 2012.
- 25 Galloway, J. N., Dentener, F. J., Capone, D. G., Boyer, E. W., Howarth, R. W., Seitzinger, S. P., Asner, G. P., Cleveland, C. C., Green, P. A., Holland, E. A., Karl, D. M., Michaels, A. F., Porter, J. H., Townsend, A. R., and Vorosmarty, C. J.: Nitrogen cycle: past, present, and future, *Biogeochemistry*, 70, 153–226, 2004.

Nitrogen and hydrological cycles under historical climate and land use

M. Lee et al.

[Title Page](#)

[Abstract](#)

[Introduction](#)

[Conclusions](#)

[References](#)

[Tables](#)

[Figures](#)

[⏪](#)

[⏩](#)

[◀](#)

[▶](#)

[Back](#)

[Close](#)

[Full Screen / Esc](#)

[Printer-friendly Version](#)

[Interactive Discussion](#)

Galloway, J. N., Townsend, A. R., Erisman, J. W., Bekunda, M., Cai, Z., Freney, J. R., Martinelli, L. A., Seitzinger, S. P., and Sutton, M. A.: Transformation of the nitrogen cycle: recent trends, questions, and potential solutions, *Science*, 320, 889–892, 2008.

Gerber, S., Hedin, L. O., Oppenheimer, M., Pacala, S. W., and Shevliakova, E.: Nitrogen cycling and feedbacks in a global dynamic land model, *Global Biogeochem. Cy.*, 24, GB1001, doi:10.1029/2008GB003336, 2010.

Green, P. A., Vorosmarty, C. J., Meybeck, M. J., Galloway, N., Peterson, B. J., and Boyer, E. W.: Pre-industrial and contemporary fluxes of nitrogen through rivers: a global assessment based on typology, *Biogeochemistry*, 68, 71–105, 2004.

Grimm, J. W. and Lynch, J. A.: Improved daily precipitation nitrate and ammonium concentration models for the Chesapeake Bay Watershed, *Environ. Pollut.*, 135, 445–455, 2005.

Hameedi, J., Paerl, H., Kennish, M., and Whittall, D.: Nitrogen deposition in US Coastal bays and estuaries, *EM: The Magazine for Environmental Managers*, December 2007, 19–25, 2007.

Heinen, M.: Simplified denitrification models: overview and properties, *Geoderma*, 133, 144–463, 2006.

Henriksen, A. and Brakke, D. F.: Increasing contributions of nitrogen to the acidity of surface waters in Norway, *Water Air Soil Poll.*, 42, 183–202, 1988.

Hoffman, J. L. R.: The 2008 Susquehanna River basin water quality assessment report, Susquehanna River Basin Commission, Harrisburg, Pennsylvania, 2008.

Hoffman, J. L. R.: Susquehanna large river assessment project, Publication 265, Susquehanna River Basin Commission, Harrisburg, Pennsylvania, 2009.

Howarth, R. W.: Nutrient over-enrichment of coastal waters in the United States: steps toward a solution, *Pew Oceans Commission*, Washington, DC, 2002.

Howarth, R. W., Swaney, D. P., Boyer, E. W., Marino, R., Jaworski, N., and Goodale, C.: The influence of climate on average nitrogen export from large watersheds in the Northeastern United States, *Biogeochemistry*, 79, 163–186, 2006.

Hurt, G. C., Frolking, S., Fearon, M. G., Moore, B., Shevliakova, E., Malyshev, S., Pacala, S. W., and Houghton, R. A.: The underpinnings of land-use history: three centuries of global gridded land-use transitions, wood-harvest activity, and resulting secondary lands, *Glob. Change Biol.*, 12, 1208–1229, 2006.

Johnsson, H., Bergstrom, L., Jansson, P., and Paustian, K.: Simulated nitrogen dynamics and losses in a layered agricultural soil, *Agr. Ecosyst. Environ.*, 18, 333–356, 1987.

Nitrogen and hydrological cycles under historical climate and land use

M. Lee et al.

[Title Page](#)

[Abstract](#)

[Introduction](#)

[Conclusions](#)

[References](#)

[Tables](#)

[Figures](#)

[⏪](#)

[⏩](#)

[◀](#)

[▶](#)

[Back](#)

[Close](#)

[Full Screen / Esc](#)

[Printer-friendly Version](#)

[Interactive Discussion](#)



- Kelly, C. A., Rudd, J. W. M., and Schindler, D. W.: Acidification by nitric acid: future Considerations, *Water Air Soil Poll.*, 50, 49–61, 1990.
- Kroes, J. G. and Roelsma, J.: User's guide for the ANIMO version 3.5 nutrient leaching Model, Technical Document 46, DLO-Staring Centrum, Wageningen, the Netherlands, 1998.
- 5 Leadley, P. W., Reynolds, J. F., and Chapin, F. S.: A model of nitrogen uptake by *Eriophorum Vaginatum* roots in the field: ecological implications, *Ecol. Monogr.*, 67, 1–22, 1997.
- Neff, J. C. and Asner, G. P.: Dissolved organic carbon in terrestrial ecosystems: synthesis and a model, *Ecosystems*, 4, 29–48, 2001.
- Leopold, L. B. and Maddock, T.: The hydraulic geometry of stream channels and some physiographic implications, *US Geol. Surv. Prof. Paper*, 252, 57 pp., 1953.
- 10 McGonigal, K. H.: 2010 nutrients and suspended sediment in the Susquehanna River basin, Susquehanna River Basin Commission, Harrisburg, Pennsylvania, 2011.
- Milly, P. C. D., Malyshev, S. L., Shevliakova, E., Dunne, K. A., Findell, K. L., Gleeson, T., Liang, Z., Phillips, P., Stouffer, R. J., and Swenson, S.: An enhanced model of land water and energy for global hydrologic and earth-system studies, *J. Hydrometeorol.*, in review, 15 2014.
- Mulholland, P. J., Helton, A. M., Poole, G. C., Hall, R. O., Hamilton, S. K., Peterson, B. J., Tank, J. L., Ashkenas, L. R., Cooper, L. W., Dahm, C. N., Dodds, W. K., Findlay, S. E. G., Gregory, S. V., Grimm, N. B., Johnson, S. L., McDowell, W. H., Meyer, J. L., Valett, H. M., Webster, J. R., Arango, C. P., Beaulieu, J. J., Bernot, M. J., Burgin, A. J., Crenshaw, C. L., Johnson, L. T., Niederlehner, B. R., O'Brien, J. M., Potter, J. D., Sheibley, R. W., Sobota, D. J., and Thomas, S. M.: Stream denitrification across biomes and its response to anthropogenic nitrate loading, *Nature*, 452, 202–205, 2008.
- Murdoch, P. S. and Stoddard, J. L.: The role of nitrate in the acidification of streams in the Catskill Mountains of New York, *Water Resour. Res.*, 28, 2707–2720, 1992.
- 25 NOAA (National Oceanic and Atmospheric Administration)'s Earth System Research Laboratory: available at: www.esrl.noaa.gov/gmd/ccgg/trends (last access: 21 February 2014), 2011.
- Nordin, A., Schmidt, I. K., and Shaver, G. R.: Nitrogen uptake by arctic soil microbes and plants in relation to soil nitrogen supply, *Ecology*, 85, 955–962, 2004.
- 30 Parton, W. J., Scurlock, J. M. O., Ojima, D. S., Gilmanov, T. G., Scholens, R. J., Schimesl, D. S., Kirchner, T., Menaut, J.-C., Seastedt, T., Moya, E. G., Kamnalrut, A., and Kinyamario, J. I.:

Nitrogen and hydrological cycles under historical climate and land use

M. Lee et al.

[Title Page](#)

[Abstract](#)

[Introduction](#)

[Conclusions](#)

[References](#)

[Tables](#)

[Figures](#)

[⏪](#)

[⏩](#)

[◀](#)

[▶](#)

[Back](#)

[Close](#)

[Full Screen / Esc](#)

[Printer-friendly Version](#)

[Interactive Discussion](#)



Observations and modeling of biomass and soil organic matter dynamics for the grassland biome worldwide, *Global Biogeochem. Cy.*, 7, 785–809, 1993.

Scavia, D., Field, J. C., Boesch, D. F., Buddemeier, R. W., Burkett, V., Canyon, D. R., Fogarty, M., Harwell, M. A., Howarth, R. W., Mason, C., Reed, D. J., Royer, T. C., Sallenger, A. H., and Titus, J. G.: Climate change impacts on US coastal and marine ecosystems, *Estuaries*, 25, 149–164, 2002.

Schilling, K. E. and Wolter, C. F.: Modeling nitrate-nitrogen load reduction strategies for the Des Moines River, Iowa using SWAT, *J. Environ. Manage.*, 44, 671–82, 2009.

Seitzinger, S. P., Styles, R. V., Boyer, E., Alexander, R. B., Billen, G., Howarth, R., Mayer, B., Van Breemen, N.: Nitrogen retention in rivers: model development and application to watersheds in the eastern US, *Biogeochemistry*, 57/58, 199–237, 2002.

Sharpley, A. N. and Williams, J. R.: EPIC erosion/productivity impact calculator: 1. Model Documentation, Technical Bulletin No. 1768, US Department of Agriculture, Temple, Texas, USA, 1990.

Sheffield, J., Goteti, G., and Wood, E. F.: Development of a 50-yr high-resolution global dataset of meteorological forcings for land surface modeling, *J. Climate*, 19, 3088–3111, 2006.

Shevliakova, E., Pacala, S. W., Malyshev, S., Hurtt, G. C., Milly, P. C. D., Caspersen, J. P., Sentman, L. T., Fisk, J. P., Wirth, C., and Crevoisier, C.: Carbon cycling under 300 years of land use changes: importance of the secondary vegetation sink, *Global Biogeochem. Cy.*, 23, GB2022, doi:10.1029/2007GB003176, 2009.

Smith, V. H.: Eutrophication of freshwater and marine ecosystems: a global problem, *Environ. Sci. Pollut. R.*, 10, 126–139, 2003.

Smith, V. H., Joye, S. B., and Howarth, R. W.: Eutrophication of freshwater and marine ecosystems, *Limnol. Oceanogr.*, 51, 351–355, 2006.

Sogn, T. A. and Abrahamsen, G.: Simulating effects of S and N deposition on soil water chemistry by the nutrient cycling model NuCM, *Ecol. Model.*, 99, 101–111, 1997.

SRBC (Susquehanna River Basin Commission): available at: <http://www.srbc.net/> (last access: 17 January 2014), 2006.

Tague, C. L. and Band, L. E.: RHESSys: regional hydro-ecologic simulation system – an object-oriented approach to spatially distributed modeling of carbon, water, and nutrient cycling, *Earth Interact.*, 8, 1–42, 2004.

Thomas, R. Q., Bonan, G. B., and Goodale, C. L.: Insights into mechanisms governing forest carbon response to nitrogen deposition: a model–data comparison using observed

Nitrogen and hydrological cycles under historical climate and land use

M. Lee et al.

Title Page

Abstract

Introduction

Conclusions

References

Tables

Figures

◀

▶

◀

▶

Back

Close

Full Screen / Esc

Printer-friendly Version

Interactive Discussion

responses to nitrogen addition, *Biogeosciences*, 10, 3869–3887, doi:10.5194/bg-10-3869-2013, 2013.

Thornton, P. E., Lamarque, J., Rosenbloom, N. A., and Mahowald, N. M.: Influence of carbon-nitrogen cycle coupling on land model response to CO₂ fertilization and climate variability, *Global Biogeochem. Cy.*, 21, GB4018, doi:10.1029/2006GB002868, 2007.

USEPA (US Environmental Protection Agency): Chesapeake Bay Phase 5.3 Community Watershed Model, EPA 903S10002 – CBP/TRS-303-10, US Environmental Protection Agency, Chesapeake Bay Program Office, Annapolis, MD, 2010a.

USEPA (US Environmental Protection Agency): Estimates of county-level nitrogen and phosphorus data for use in modeling pollutant reduction: documentation for Scenario Builder Version 2.2. CBP/TRS 903R100004 Bin # 304, US Environmental Protection Agency Chesapeake Bay Program Office, Annapolis, MD, 2010b.

USGS (US Geological Survey): available at: <http://www.usgs.gov/> (last access: 17 January 2014), 2009.

Van Breemen, N., Boyer, E. W., Goodale, C. L., Jaworski, N. A., Paustian, K., Seitzinger, S., Lajtha, L. K., Mayer, B., Van Dam, D., Howarth, R. W., Nadelhoffer, K. J., Eve, M., Billen, G.: Where did all the nitrogen go? Fate of nitrogen inputs to large watersheds in the northeastern USA, *Biogeochemistry*, 57/58, 267–293, 2002.

Wade, A. J., Durand, P., Beaujouan, V., Wessel, W. W., Raat, K. J., Whitehead, P. G., Butterfield, D., Rankinen, K., and Lepisto, A.: A nitrogen model for European catchments: INCA, new model structure and equations, *Hydrol. Earth Syst. Sci.*, 6, 559–582, doi:10.5194/hess-6-559-2002, 2002.

Williams, J. R.: The EPIC model, in: *Computer Models of Watershed Hydrology*, edited by: Singh, V. P., Water Resources Publications, Highlands Ranch, Colorado, USA, 1995.

Table 2. Variable list in the equations.

Variable	Description	Unit
Variables in the land component equations		
C_{LF}, C_{LS}, C_{SS}	fast litter, slow litter, slow soil C contents	kg m^{-2}
D_N	soil denitrification rate	$\text{kg m}^{-2} \text{yr}^{-1}$
D_s	water drainage from active soil layer	$\text{kg m}^{-2} \text{s}^{-1}$
f_{LF}, f_{LS}, f_{SS}	fractions of soluble organic N in the fast litter, slow litter, slow soil N pools Gerber et al. (2010)	unitless
f_S	soil water content reduction function	unitless
f_T	soil temperature reduction function	unitless
h_s	effective soil depth	m
$L_{DON}, L_{NH_4^+}, L_{NO_3^-}$	soil leaching for DON, ammonium-N, nitrate-N	$\text{kg m}^{-2} \text{s}^{-1}$
$[N_{DON,av}], [N_{NH_4^+,av}], [N_{NO_3^-,av}]$	concentration of available N in DOM, ammonium-N, nitrate-N pools	kg m^{-3}
N_{LF}, N_{LS}, N_{SS}	fast litter, slow litter, slow soil N contents	kg m^{-2}
$N_{NH_4^+}, N_{NO_3^-}$	soil ammonium-N, nitrate-N contents	kg m^{-2}
S	soil water content	unitless
T	soil temperature	$^{\circ}\text{C}$
Variables in the river component equations		
$C_{NO_3^-}$	nitrate-N concentration	$\mu\text{mol NL}^{-1}$
f_T'	stream temperature reduction function	unitless
$F_{DON}^{in}, F_{NH_4^+}^{in}, F_{NO_3^-}^{in}$	river inflow of DON, ammonium-N, nitrate-N	$\text{kg m}^{-2} \text{s}^{-1}$
$F_{DON}^{out}, F_{NH_4^+}^{out}, F_{NO_3^-}^{out}$	river outflow of the DON, ammonium-N, nitrate-N	$\text{kg m}^{-2} \text{s}^{-1}$
H	river depth	m
k_{denitr}	reaction rate constant for river denitrification	s^{-1}
$P_{DON}, P_{NH_4^+}, P_{NO_3^-}$	point sources of DIN, ammonium-N, nitrate-N	$\text{kg m}^{-2} \text{s}^{-1}$
$R_{DON}, R_{NH_4^+}, R_{NO_3^-}$	DON, ammonium-N, nitrate-N in rivers	kg m^{-2}
T'	water temperature	$^{\circ}\text{C}$

Nitrogen and hydrological cycles under historical climate and land use

M. Lee et al.

Title Page

Abstract

Introduction

Conclusions

References

Tables

Figures

◀

▶

◀

▶

Back

Close

Full Screen / Esc

Printer-friendly Version

Interactive Discussion

Nitrogen and hydrological cycles under historical climate and land use

M. Lee et al.

Table 3. Susquehanna River Basin Geographic Statistics for the SRBC nutrient monitoring sites (McGonigal, 2011).

Site Location	Waterbody	Sub basin Area, km ²	2000 Land Use Percentages					
			Water/Wetland	Urban	Agricultural Cropland	Pasture	Forest	Other
6 Long-term Sites								
Towanda 1989~	Susquehanna	20 194	2	5	17	5	71	0
Danville 1985~	Susquehanna	29 060	2	6	16	5	70	1
Lewisburg 1985~	W B Susque	17 734	1	5	8	2	84	0
Newport 1985~	Juniata	8687	1	6	14	4	74	1
Marietta 1987~	Susquehanna	67 314	2	7	14	5	72	0
Conestoga 1985~	Conestoga	1217	1	24	12	36	26	1
9 Newly Introduced Sites								
Conklin 2005~	Susquehanna	5778	3	3	18	4	71	1
Smithboro 2004~	Susquehanna	11 989	3	5	17	5	70	0
Campbell 2005~	Cohocton	1217	3	4	13	6	74	0
Chemung 2004~	Chemung	6488	2	5	15	5	73	0
Wilkes-Barre 2004~	Susquehanna	25 785	2	6	16	5	71	0
Karthus 2004~	W B Susque	3785	1	6	11	1	80	1
Castanea 2004~	Bald Eagle	1087	1	8	11	3	76	1
Saxton 2004~	Raystown B Juni	1957	< 0.5	6	18	5	71	0
Manchester 2004~	W Conewago	1320	2	13	12	36	36	1

[Title Page](#)
[Abstract](#)
[Introduction](#)
[Conclusions](#)
[References](#)
[Tables](#)
[Figures](#)
[Back](#)
[Close](#)
[Full Screen / Esc](#)
[Printer-friendly Version](#)
[Interactive Discussion](#)

Nitrogen and hydrological cycles under historical climate and land use

M. Lee et al.

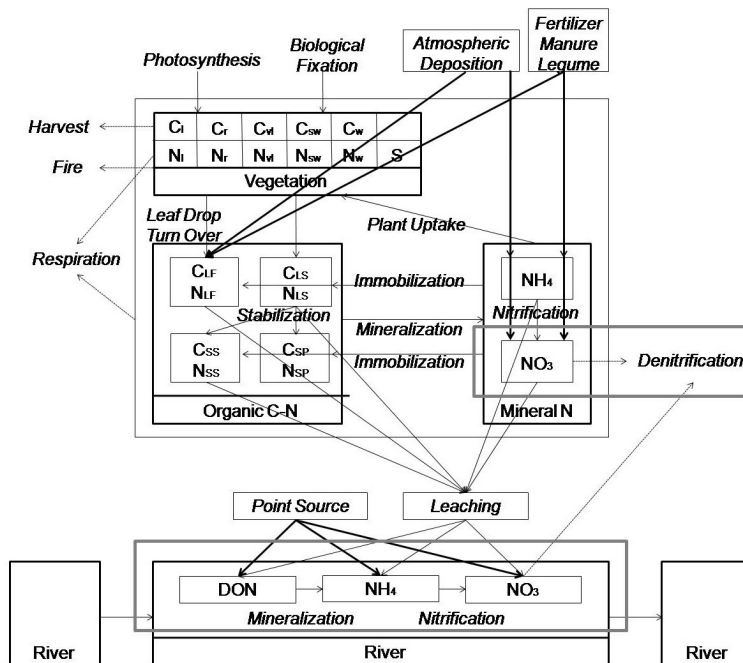


Fig. 1. Structure of LM3-TAN. Two thick boxes show the incorporated denitrification module in the terrestrial component and stream microbial processes in the river component. The river systems are a series of continuously stirred tank reactors (CSTR) that simulate stream mineralization, nitrification, and denitrification. The other boxes show major C and N pools in vegetation (leaves, fine roots, labile, sapwood, heartwood, and N buffer storage), soil (fast and slow little, slow and passive soil, mineral N), and river (organic and mineral N). The arrows depict fluxes of anthropogenic N sources (thick solid), C-N organic compounds and mineral N (thin solid) with associated processes (italic), and C and N lost to the atmosphere or anthropogenic pool (dashed).

Title Page	
Abstract	Introduction
Conclusions	References
Tables	Figures
◀	▶
◀	▶
Back	Close
Full Screen / Esc	
Printer-friendly Version	
Interactive Discussion	

Nitrogen and hydrological cycles under historical climate and land use

M. Lee et al.

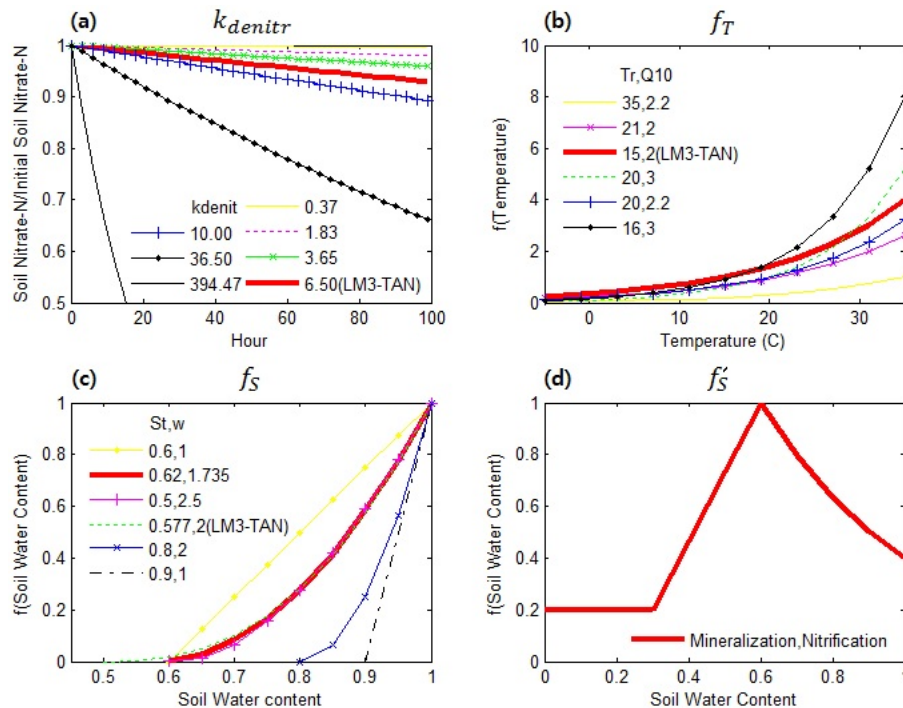


Fig. 2. Overview of the denitrification module. Effects of first-order denitrification coefficient **(a)**, soil temperature reduction function **(b)**, soil water content reduction function **(c)** on soil denitrification rate; soil water content reduction function for mineralization and nitrification **(d)**. The curves were produced using the Tables 3, 6, and 7 in Heinen (2006).

Title Page

Abstract

Introduction

Conclusions

References

Tables

Figures

◀

▶

◀

▶

Back

Close

Full Screen / Esc

Printer-friendly Version

Interactive Discussion

Nitrogen and hydrological cycles under historical climate and land use

M. Lee et al.



Fig. 3. Map of the Susquehanna watershed, showing 6 major sub-basins, main stem of the Susquehanna River, major tributaries (Chemung, West Branch Susquehanna, and Juniata River), streams, and the location of USGS stream gauges and SRBC nutrient monitoring sites.

Title Page

Abstract

Introduction

Conclusions

References

Tables

Figures

◀

▶

◀

▶

Back

Close

Full Screen / Esc

Printer-friendly Version

Interactive Discussion

Nitrogen and hydrological cycles under historical climate and land use

M. Lee et al.

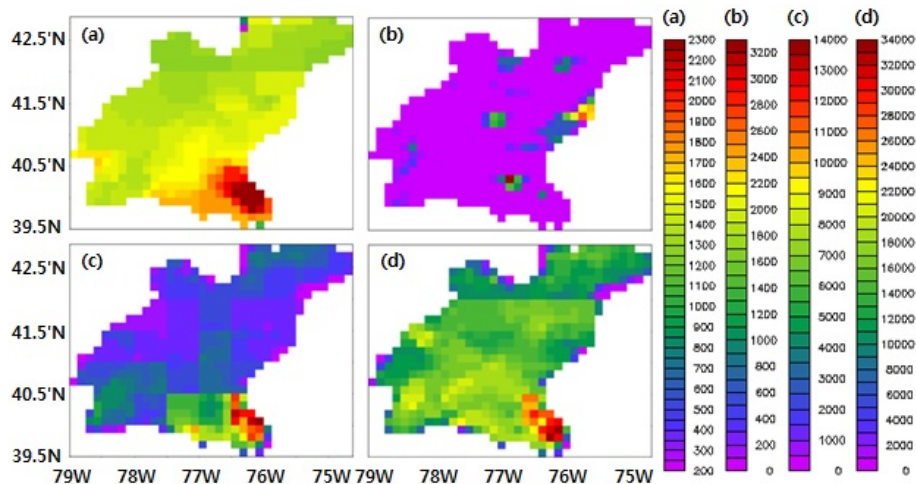


Fig. 4. Spatial distribution maps of the applied 20 year (1986–2005) average anthropogenic N sources: atmospheric deposition ($\text{kg km}^{-2} \text{yr}^{-1}$) (a), combined sewer overflow (b), and fertilizer, manure, and legume applications ($\text{kg km}^{-2} \text{yr}^{-1}$) (c) and ($\text{kg cropland km}^{-2} \text{yr}^{-1}$) (d).

[Title Page](#)

[Abstract](#)

[Introduction](#)

[Conclusions](#)

[References](#)

[Tables](#)

[Figures](#)

⏪

⏩

◀

▶

[Back](#)

[Close](#)

[Full Screen / Esc](#)

[Printer-friendly Version](#)

[Interactive Discussion](#)



Nitrogen and hydrological cycles under historical climate and land use

M. Lee et al.

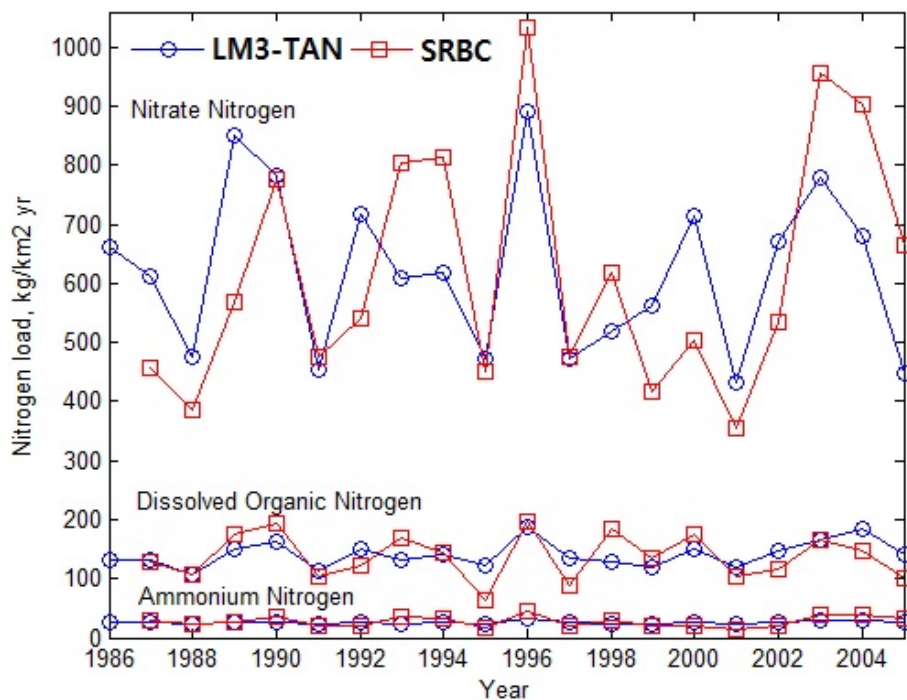


Fig. 5. 19 years (1987–2005) of the simulated stream N loads at Marietta and the corresponding observed data from SRBC.

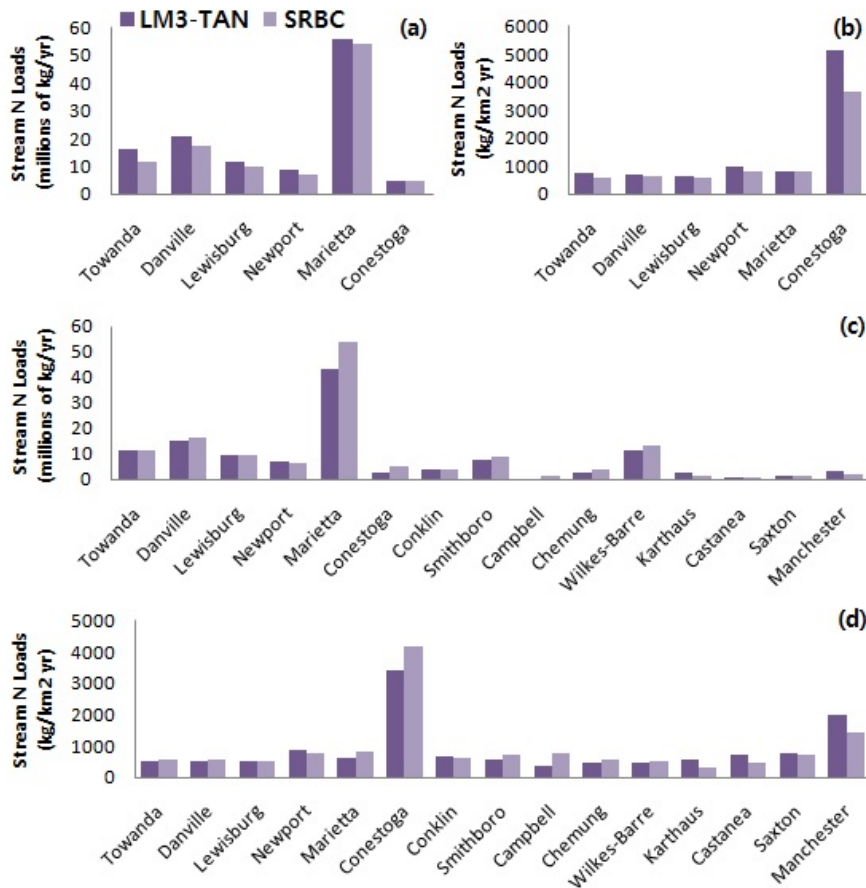


Fig. 6. 17 year (1989–2005) average simulated and reported (SRBC) stream N loads at the 6 long-term monitoring sites in **(a)** millions of kg yr^{-1} and **(b)** $\text{kg km}^{-2} \text{ yr}$; simulated and reported stream N loads for the year 2005 at the 15 monitoring sites in **(c)** millions of kg yr^{-1} and **(d)** $\text{kg km}^{-2} \text{ yr}$.

Title Page

Abstract Introduction

Conclusions References

Tables Figures

◀ ▶

◀ ▶

Back Close

Full Screen / Esc

Printer-friendly Version

Interactive Discussion

Nitrogen and hydrological cycles under historical climate and land use

M. Lee et al.

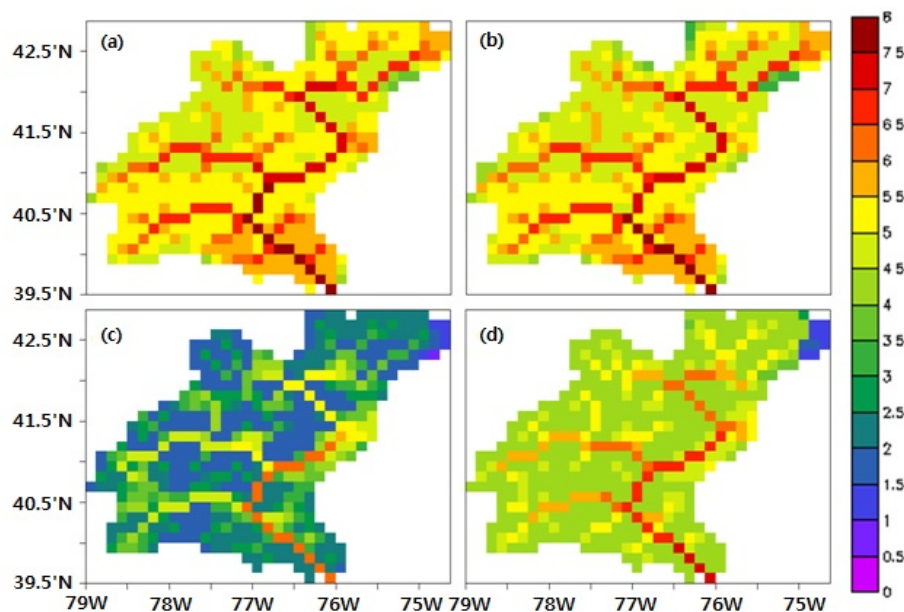


Fig. 7. Spatial distribution maps of 20 year (1986–2005) average simulated stream **(a)** dissolved N, **(b)** nitrate N, **(c)** ammonium N, and **(d)** dissolved organic N loads, log(kgyr⁻¹).

[Title Page](#)[Abstract](#)[Introduction](#)[Conclusions](#)[References](#)[Tables](#)[Figures](#)[◀](#)[▶](#)[◀](#)[▶](#)[Back](#)[Close](#)[Full Screen / Esc](#)[Printer-friendly Version](#)[Interactive Discussion](#)

Nitrogen and hydrological cycles under historical climate and land use

M. Lee et al.

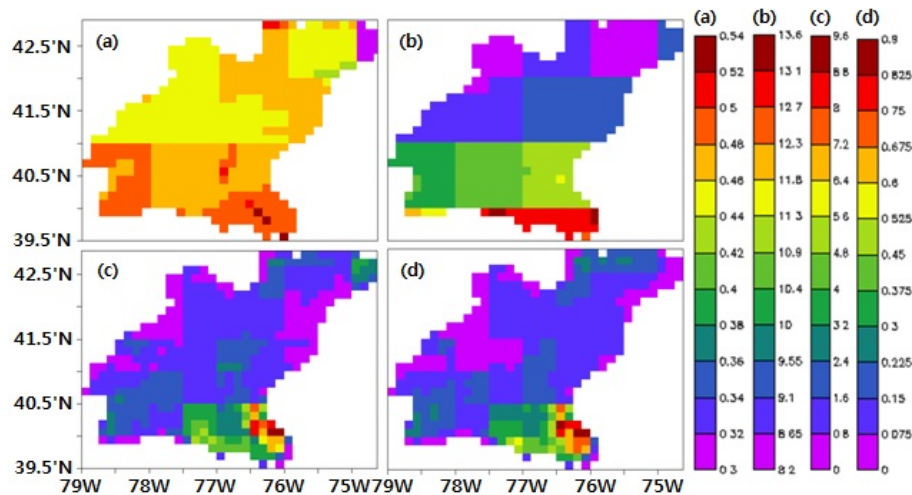


Fig. 8. Spatial distribution maps of 20 year average (1986–2005) **(a)** soil water content, **(b)** temperature ($^{\circ}\text{C}$), **(c)** nitrate N content ($10^2 \times \text{kgm}^{-2} \text{yr}^{-1}$), and **(d)** denitrification rate ($10^2 \times \text{kgm}^{-2} \text{yr}^{-1}$).

[Title Page](#)

[Abstract](#)

[Introduction](#)

[Conclusions](#)

[References](#)

[Tables](#)

[Figures](#)

[⏪](#)

[⏩](#)

[◀](#)

[▶](#)

[Back](#)

[Close](#)

[Full Screen / Esc](#)

[Printer-friendly Version](#)

[Interactive Discussion](#)



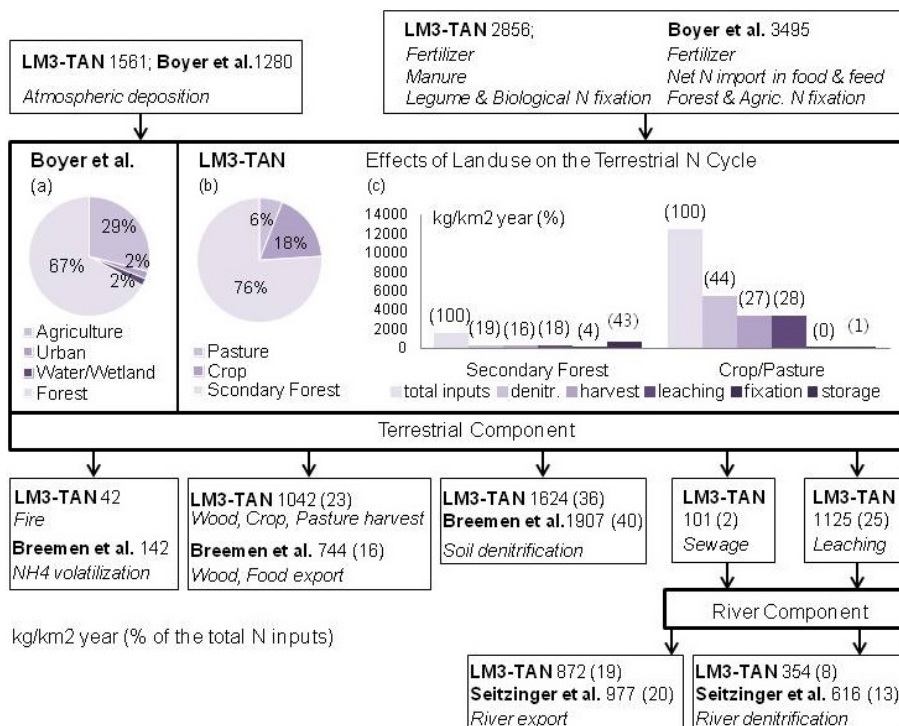


Fig. 9. Comparison between the calculated and reported budgets of N sources, retention, lost, transport, and river export at the level of the whole Susquehanna watershed for the period 1988 to 1992 (Boyer et al., 2002; Breemen et al., 2002; Seitzinger et al., 2002; USEPA, 2010a).

Nitrogen and hydrological cycles under historical climate and land use

M. Lee et al.

[Title Page](#)

[Abstract](#)

[Introduction](#)

[Conclusions](#)

[References](#)

[Tables](#)

[Figures](#)

[⏪](#)

[⏩](#)

[◀](#)

[▶](#)

[Back](#)

[Close](#)

[Full Screen / Esc](#)

[Printer-friendly Version](#)

[Interactive Discussion](#)

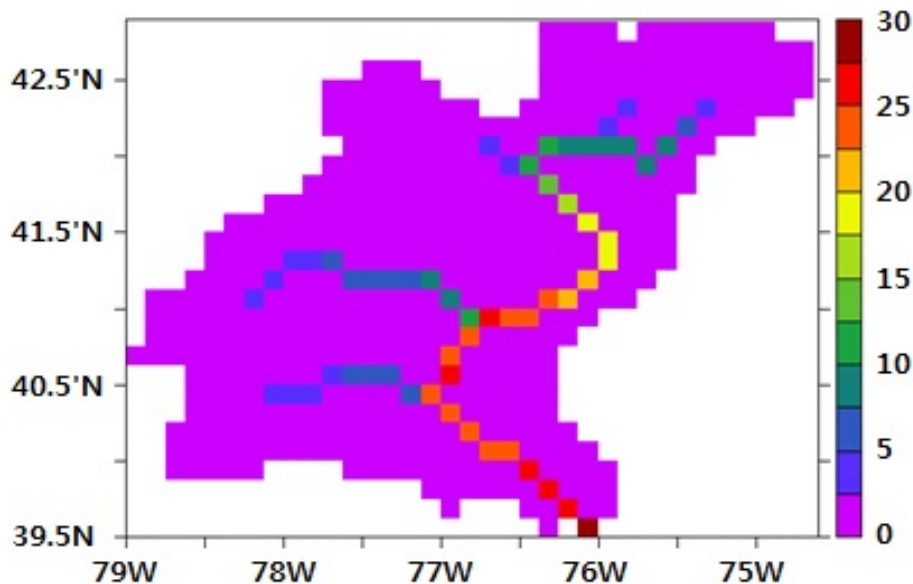


Fig. 10. N removal by river denitrification (%) = (river N load with “ $k_{\text{denitr}}' = 0$ ” – river N load with “estimated k_{denitr}' ”)/river N load with “ $k_{\text{denitr}}' = 0$ ” $\times 100$.